



**Queensland University of Technology**  
Brisbane Australia

This is the author's version of a work that was submitted/accepted for publication in the following source:

Zhang, Shuai, Liu, Qinfu, Cheng, Hongfei, Li, Xiaoguang, Zeng, Fangui, & [Frost, Ray L.](#)

(2014)

Intercalation of dodecylamine into kaolinite and its layering structure investigated by molecular dynamics simulation.

*Journal of Colloid and Interface Science*, 430, pp. 345-350.

This file was downloaded from: <https://eprints.qut.edu.au/73139/>

© Copyright 2014 Elsevier Inc.

This is the author's version of a work that was accepted for publication in *Journal of Colloid and Interface Science*. Changes resulting from the publishing process, such as peer review, editing, corrections, structural formatting, and other quality control mechanisms may not be reflected in this document. Changes may have been made to this work since it was submitted for publication. A definitive version was subsequently published in *Journal of Colloid and Interface Science*, [VOL 430, (2014)] DOI: 10.1016/j.jcis.2014.05.059

**Notice:** *Changes introduced as a result of publishing processes such as copy-editing and formatting may not be reflected in this document. For a definitive version of this work, please refer to the published source:*

<https://doi.org/10.1016/j.jcis.2014.05.059>

# Intercalation of dodecylamine into kaolinite and its layering structure investigated by molecular dynamics simulation

Shuai Zhang <sup>a</sup>, Qinfu Liu <sup>a\*</sup>, Hongfei Cheng <sup>a</sup>, Xiaoguang Li <sup>a</sup>, Fangui Zeng <sup>b</sup>,  
Ray L. Frost <sup>c\*</sup>

<sup>a</sup> School of Geoscience and Surveying Engineering, China University of Mining & Technology, Beijing, 100083, China

<sup>b</sup> Department of Earth Science and Engineering, Taiyuan University of Technology, Taiyuan, 030024, China

<sup>c</sup> School of Chemistry, Physics and Mechanical Engineering, Science and Engineering Faculty, Queensland University of Technology, 2 George Street, GPO Box 2434, Brisbane, Queensland 4001, Australia

Corresponding author: **Qinfu Liu**

Fax: +86 10 62331248,

E-mail addresses: [lqf@cumtb.edu.cn](mailto:lqf@cumtb.edu.cn)

Corresponding author: **Ray L. Frost**

Fax: +61 7 3138 2407,

E-mail addresses: [r.frost@qut.edu.au](mailto:r.frost@qut.edu.au)

---

\* Corresponding authors. Fax: +86 10 62331248 (Q. Liu) , +61 7 3138 2407 (R. L. Frost)  
E-mail addresses: [lqf@cumtb.edu.cn](mailto:lqf@cumtb.edu.cn) (Q. Liu), [r.frost@qut.edu.au](mailto:r.frost@qut.edu.au) (R. L. Frost)

**Abstract:** Dodecylamine was successfully intercalated into the layer space of kaolinite by utilizing the methanol treated kaolinite- dimethyl sulfoxide (DMSO) intercalation complex as an intermediate. The basal spacing of kaolinite, measured by X-ray diffraction (XRD), increased from 0.72 nm to 4.29 nm after the intercalation of dodecylamine. Also, the significant variation observed in the Fourier Transform Infrared Spectroscopy (FTIR) spectra of kaolinite when intercalated with dodecylamine verified the feasibility of intercalation of dodecylamine into kaolinite. Isothermal-isobaric (NPT) molecular dynamics simulation with the use of Dreiding force field was performed to probe into the layering behavior and structure of nanoconfined dodecylamine in the kaolinite gallery. The concentration profiles of the nitrogen atom, methyl group and methylene group of intercalated dodecylamine molecules in the direction perpendicular to the kaolinite basal surface indicated that the alkyl chains within the interlayer space of kaolinite exhibited an obvious layering structure. However, the unified bilayer, pseudo-trilayer, or paraffin-type arrangements of alkyl chains deduced on the basis of their chain length combined with the measured basal spacing of organoclays were not found in this study. The alkyl chains aggregated to a mixture of ordered paraffin-type-like structure and disordered gauche conformation in the middle interlayer space of kaolinite, and some alkyl chains arranged in two bilayer structures, in which one was close to the silica tetrahedron surface, and the other was close to the alumina octahedron surface with their alkyl chains parallel to the kaolinite basal surface.

**Keywords:** Kaolinite, Intercalation, Dodecylamine, Molecular dynamics simulation, Layering structure

## 1. Introduction

Orgnoclays, generally defined as organic modified clays, are widely applied in various industries due to their special modified surface characters, including the rheological controlling of paints and greases, selective absorption for toxic pollutants, preparation of polymer nanocomposites, etc. [1, 2]. Orgnoclays are usually synthesized through intercalation of clays with organic surfactants, which results in the transition of clay surface from hydrophilic to organophilic. Thus, the modified clays are able to disperse into the polymer matrix to generate novel polymer/clay nanocomposites, which exhibit significantly improved properties on tensile strength, thermostability, barrier performance, and flame retardance compared to those pristine polymers. Layered solids such as clay minerals have been proven to be an ideal host material for the synthesis of orgnoclays by intercalating with organic surfactants in the form of liquids, melts, or concentrated solutions. In previous studies, smectite groups of clay minerals have been investigated extensively as hosts because of their attractive features on swelling behavior, large surface area, and cationic exchangeability [3-10]. Kaolinite, a layer silicate mineral, consists of nanometer thick layers formed by stacking an aluminum octahedron sheet and a silicon tetrahedron sheet along the direction perpendicular to its (001) crystal plane. Unlike montmorillonite, the crystalline network of kaolinite is practically devoid of isomorphic substitutions, so it does not require charge compensation of hydrated interlayer cations, thus, it lacks the expansion behavior and the exchangeable cations in its interlayer space. In addition, the layers in kaolinite are held together by hydrogen

bonds, dipole-dipole interactions, and van der Waals forces. These characteristics cause the intercalation of kaolinite with guest molecules to be difficult. However, a limited number of high polar organic species such as urea [11, 12], dimethyl sulfoxide [13], formamide [14], hydrazine [15], and potassium acetate [16-19] have been validated that they can be successfully intercalated into the kaolinite gallery. Those intercalated derivatives can serve as a precursor for preparing kaolinite-surfactant organoclays, but which are hard to prepare through displacing the preintercalated small molecules with organic surfactants in a direct replacing intercalation method. While a process usually called indirection method has been applied for preparations of several kinds of kaolinite-based organoclays [20-25]. Compared with montmorillonite, Kaolinite presents excellent performance when used as nanofiller in the fabrication of polymer/clay nanocomposites due to its perfect layer structure, less impurity, and substantial deposits in China. Understanding the structure of organoclays and the interaction between kaolinite and surfactants is of significance in design and characterization of polymer/clay nanocomposites. So far, XRD is the most common used technique to determine the layered structure and orientation of intercalated species, which has been applied by Kuroda et al. [24] and Gardolinski et al. [23] to study the structure of kaolinite-alkylamines intercalation compounds. On the basis of the relation between their basal spacings and the length of alkyl chains, they inferred that the alkyl chains were fully stretched (all-trans conformation) and perpendicular to the basal plane surface, and arranged in a bilayer between the kaolinite layers.

Although various structural models have been proposed for the intercalated surfactant, significant structural characteristics of the surfactants, i.e. trans and gauche conformations have not been directly revealed. Molecular dynamics simulation has proven to be an effective technique for a further insight into the structural characteristics in the nano-confined environment. To date, only a few MD simulation studies about the intercalation of kaolinite with some small molecules have been reported [26-28]. As far as we know, almost no investigations on modeling macromolecular surfactants intercalated into the kaolinite gallery have been reported. In this study, the intercalation of kaolinite with dodecylamine was investigated by using the X-ray Diffraction (XRD) and Fourier Transform Infrared Spectroscopy (FTIR). In addition, molecular dynamics simulation was employed to probe the layer behavior and interlayer structure of dodecylamine confined between the layers of kaolinite at a molecular level. The atomic density profiles and configuration of alkyl chains were produced and discussed.

## **2. Experimental**

### *2.1 Materials*

The kaolinite used in the present study was natural pure kaolinite with the size of 45  $\mu\text{m}$  from Zhangjiakou, Hebei Province, China. The chemical composition of the sample in mass % was:  $\text{SiO}_2$ , 44.64;  $\text{Al}_2\text{O}_3$ , 38.05;  $\text{Fe}_2\text{O}_3$ , 0.22;  $\text{MgO}$ , 0.06;  $\text{CaO}$ , 0.11;  $\text{Na}_2\text{O}$ , 0.27;  $\text{K}_2\text{O}$ , 0.08;  $\text{TiO}_2$ , 1.13;  $\text{P}_2\text{O}_5$ , 0.13;  $\text{MnO}$ , 0.002; and loss on ignition,

15.06. The major mineral constituent was a well-ordered kaolinite (95 mass %) with a Hinckley index of approximately 1.31. All reagents were purchased from Xilong Chemical Company, Ltd. (China) in purities of at least 98 % and used without further treatment.

## *2.2. Preparation of kaolinite intercalation complex*

The kaolinite intercalation complex with dodecylamine was prepared by the indirect intercalation reaction mentioned above. Firstly, intercalation complex with dimethylsulfoxide (DMSO) as the first intermediate was prepared by adding 50 g kaolinite into a closed container that contained 90 ml DMSO and 10 ml deionized water. The mixture was stirred with the magnetic stirrer at 60 °C for 12 h, and then the suspension was separated by centrifugation with ethyl alcohol. Secondly, after drying the prepared DMSO intercalated samples for 24 h at 60 °C, then dispersing 5 g dried DMSO intercalated samples in 120 ml methanol for preparing the methanol-treated kaolinite. The reaction mixture was stirred with the magnetic stirrer for ten days at room temperature, and the methanol was refreshed every day. Lastly, the dodecylamine intercalation complex was prepared by stirring the mixture of dodecylamine, methanol, and wet methanol-treated kaolinite at 40 °C for 24 h. After centrifugation, the products were dried at room teomperature and analyzed by XRD and FTIR.

## *2.3. Characterization*



The XRD analyses of the prepared samples were carried out on a Rigaku D/max 2500PC X-ray diffractometer (Japan) with Cu ( $\lambda=1.54178 \text{ \AA}$ ) irradiation at the scanning rate of  $2^\circ/\text{min}$  operating at 40 kV and 150 mA. The original kaolinite, kaolinite-DMSO intercalation complex, kaolinite-methanol intercalation complex, and crystalline dodecylamine were scanned in the  $2\theta$  range of  $2^\circ$  to  $45^\circ$ , and the kaolinite-dodecylamine intercalation complex was scanned in the  $2\theta$  range of  $1^\circ$  to  $45^\circ$ .

FTIR was performed on a Thermofisher Nicolet 6700 spectrometer (USA). The FTIR spectra of the prepared samples were obtained within the range of  $400 \text{ cm}^{-1}$  to  $4000 \text{ cm}^{-1}$  in KBr pellet form (2 mg sample in 300 mg KBr).

#### *2.4. Models and simulation details*

Based on the data of Young and Hewat [29], The unite cell of kaolinite with the chemical composition of  $\text{Al}_4\text{Si}_4\text{O}_{10}(\text{OH})_8$  was built as a basic cell for the simulation. The unit cell exhibited P1 symmetry with the following lattice parameters:  $a = 0.515 \text{ nm}$ ,  $b = 0.893 \text{ nm}$ ,  $c = 0.738 \text{ nm}$ ,  $\alpha = 91.93^\circ$ ,  $\beta = 105.04^\circ$ , and  $\gamma = 89.79^\circ$ . The periodic MD simulation supercell consisted of 16 ( $4 \times 4 \times 1$ ) unite cells with a total of 544 atoms was created. The supercell has an overall size of  $a = 2.060 \text{ nm}$ ,  $b = 3.574 \text{ nm}$ . All dodecylamine molecules were packed in a cubic box with the lengths  $a$  and  $b$  matching pretty well with the constructed supercell of kaolinite. Thus they could be stacked upon each other to form a kaolinite-dodecylamine complex system for the following simulations. The Dreiding force field was adopted for these simulations, which was successfully used in the simulations of mineral-organic interfaces by

previous studies[2, 30]. The partial charges of atoms in kaolinite framework were adopted directly from the studies by Fang et al. [26]. The atomic charges of dodecylamine were assigned by a charge equilibration method [31].

The MD simulations were carried out employing Forcite program (Material Studio 4.1; Accelrys, San Diego, CA, USA) [32] on the supercomputer. All simulations were performed in the NPT ensemble for 500 ps with the pressure fixed at 0.1 Mpa and the temperature fixed at 298 K. The first 200 ps run were chosen to ensure that the system reached equilibrium, and the last 300 ps run were used to collect data for later analyses. Periodic boundary conditions were applied in three dimensions. The velocity Verlet algorithm with a time step of 1 fs was used to integrate the particle motion. The trajectory frame was recorded every 20 fs. The long-range electronic interactions were calculated by the Ewald summation method. Temperature and pressure were maintained by using the Nose thermostat and Berendsen barostat, respectively. During the simulations the Cartesian position of atoms of kaolinite were constrained in the x and y direction, but all atoms of dodecylamine molecules were allowed to freely move.

### **3. Results and discussion**

#### *3.1. XRD analysis*

Fig. 1a represents the typical XRD pattern of raw kaolinite with a (001) reflection peak of 0.72nm at low  $2\theta$  side, and a (002) reflection peak of 0.36nm. The XRD

pattern, shown in Fig. 1b, clearly presents that the basal spacing of kaolinite increases from 0.72nm to 1.12nm after the intercalation with DMSO, indicating that the DMSO has been successively intercalated into the kaolinite gallery and caused its structural expansion along the direction perpendicular to the (001) lattice plane. It is worth noting that the (020), ( $\overline{1}10$ ), ( $\overline{1}11$ ), (003), ( $\overline{2}02$ ), and (131) reflection peaks of original kaolinite in the middle-2 $\theta$  and high-2 $\theta$  regions almost disappear, thus suggesting that the well crystallized kaolinite suffered significantly structural degradation after the intercalation action. Methanol cannot be directly intercalated into the interlayer space of kaolinite. However, it can be intercalated when the kaolinite-DMSO intercalation complex is used as an intermediate. Fig. 1c shows that after the washing treatment of kaolinite-DMSO intercalation complex with methanol, the basal spacing slightly decreased to 0.89 nm. In addition, the (001) reflection peak broadens obviously. Thus, we can suggest that the indirect intercalation involving in the displacement of DMSO between the layers of kaolinite with the methanol results in a further structural degradation of kaolinite. As shown by diffraction pattern (Fig. 1d), the basal spacing of kaolinite-dodecylamine intercalation complex increases to 4.29 nm from 0.89 nm of the kaolinite-methanol intercalation complex, indicating that dodecylamine can be intercalated into the interlayer space of kaolinite by using the methanol-treated kaolinite-DMSO intercalation complex as the precursor. Moreover, a sharp reflection peak next to the peak of 4.29 nm and some other unobvious peaks at the low 2 $\theta$  value are also observed in the Fig. 1d, which are attributed to a certain amount of free

recrystalline dodecylamine. It is assumed that some dodecylamine molecules may spontaneously deintercalate from the kaolinite interlayer and recrystallize during the air drying treatment of dodecylamine intercalated products.

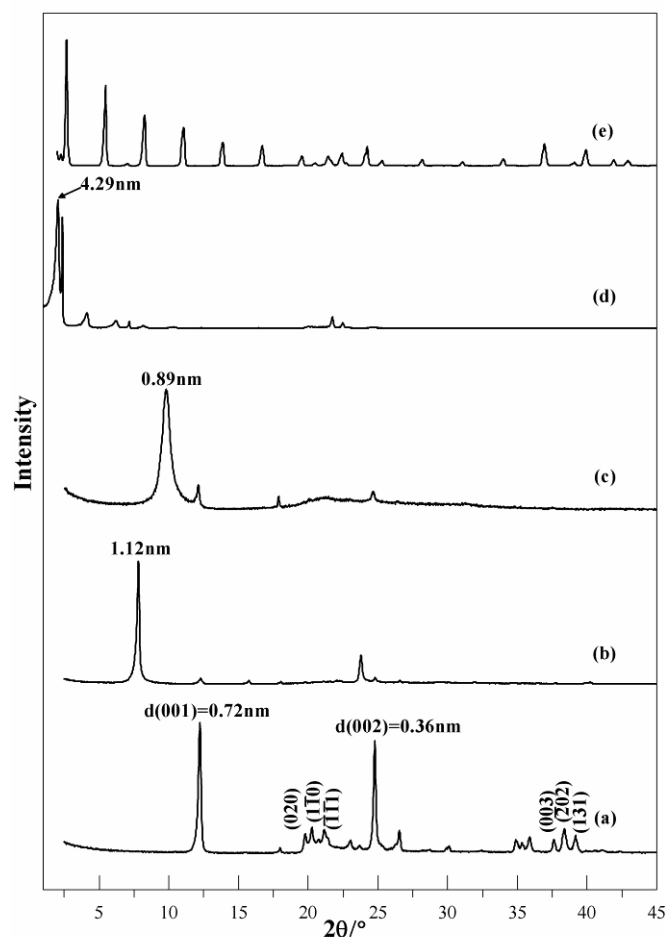


**Fig. 1.** XRD patterns of (a) original kaolinite, (b) kaolinite-DMSO intercalation complex, (c) kaolinite-methanol intercalation complex, (d) kaolinite-dodecylamine intercalation complex, and (e) crystalline dodecylamine.

### 3.2. FTIR analysis

The FTIR spectrum of the raw kaolinite in the high frequency region is shown in Fig.

2a. The three bands at  $3690$ ,  $3668$ , and  $3651\text{ cm}^{-1}$  are assigned to the OH stretching of inner surface hydroxyl, and the band at  $3620\text{ cm}^{-1}$  is assigned to the OH stretching of inner hydroxyl [33-36]. The FTIR OH stretching region of inner surface hydroxyl of kaolinite is very sensitive to the effects of interlayer modification [37, 38]. Thus,

the FTIR spectra deformation in such region is commonly used to diagnose if the intercalation guests break the original hydrogen bonds linking the kaolinite platelet, and walk into the kaolinite gallery and form new hydrogen bonds with the surface groups of kaolinite such as hydroxyl groups or oxygen atoms of the six-membered ring. However, the inner hydroxyl groups of all samples cannot be perturbed because of their particular location within the kaolinite structure. From the Fig. 2 b, c and d, it is readily observed that the OH stretching patterns are very different from that of untreated kaolinite (Fig. 2a). After the intercalation of MDSO, the FTIR spectrum of the intercalated kaolinite exhibits profound changes in the OH stretching region. As shown in Fig. 2b, the OH stretching band of inner surface hydroxyl at  $3690\text{ cm}^{-1}$  is apparently weakened, and the bands at  $3668$  and  $3651\text{ cm}^{-1}$  even disappear, but a new band at  $3659\text{ cm}^{-1}$  is detected. Additionally, in the lower wave numbers, two bands at  $3535\text{ cm}^{-1}$  and  $3500\text{ cm}^{-1}$  are also observed. Johnston et al [39] reported that the two bands at  $3535\text{ cm}^{-1}$  and  $3500\text{ cm}^{-1}$  in the FTIR spectrum of kaolinite -DMSO intercalation complex indicated clearly that the intercalated DMSO molecules formed hydrogen bonds with the inner-surface hydroxyl groups of kaolinite, which corresponded to the stretching frequency of coupled inner-surface hydroxyl groups perpendicular to the (001) plane hydrogen bonded to  $\text{S}=\text{O}$  groups of DMSO molecules in the interlamellar region. The band at  $3659\text{ cm}^{-1}$  was related to the  $3668\text{ cm}^{-1}$  band in the spectrum of nonintercalated kaolinite. However, some studies [40-42] reported that the two bands at  $3535\text{ cm}^{-1}$  and  $3500\text{ cm}^{-1}$  were assigned to the OH

stretching motion of water intercalated together with DMSO molecules as the water plays a significant role in the intercalation of DMSO into the kaolinite. And the additional band at  $3659\text{ cm}^{-1}$  was attributed to the stretching motion of inner-surface hydroxyls hydrogen bonded to the S=O groups of DMSO molecules. In all, the significant changes in the OH stretching region (Fig. 2b) suggest that the DMSO successfully intercalated into the kaolinite. After the methanol treatment, the bands at  $3659\text{ cm}^{-1}$ ,  $3535\text{ cm}^{-1}$  and  $3500\text{ cm}^{-1}$  of kaolinite-DMSO intercalation complex disappear, and a band at  $3536\text{ cm}^{-1}$  is clearly detected (Fig. 2c). These variations of peaks indicate that the hydrogen bonds formed between the inner-surface hydroxyl groups of kaolinite and the intercalated guests changed during the methanol treatment process. Thus, it is concluded that the intercalated DMSO can be replaced by the methanol through methanol washing treatment, which is also evidenced by XRD analyses described above. The band at  $3536\text{ cm}^{-1}$  is characteristic for hydrated kaolinite [43, 44], indicating that the hydrogen bonds formed between OH groups of kaolinite and water molecules are present. The major difference between the FTIR spectra of kaolinite-dodecylamine intercalation complex (Fig. 2d) and methanol-treated kaolinite-DMSO intercalation complex (Fig. 2c) is the shift of the band from  $3536\text{ cm}^{-1}$  to  $3545\text{ cm}^{-1}$ , which is due to the variation of hydrogen bonds between OH groups of kaolinite and water molecules caused by the intercalation of dodecylamine.

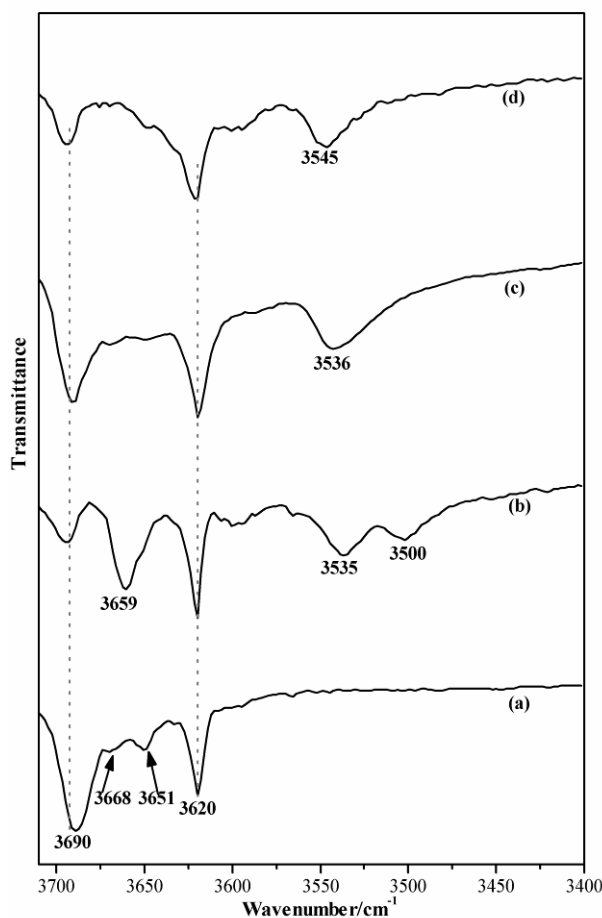


**Fig. 2.** FTIR spectra of (a) kaolinite, (b) kaolinite-DMSO intercalation complex, (c) methanol-treated kaolinite-DMSO intercalation complex, and (d) kaolinite-dodecylamine intercalation complex in the high frequency region.

The FTIR spectrum of the kaolinite-dodecylamine intercalation complex in the middle frequency region is shown in Fig. 3. The band at  $1566\text{ cm}^{-1}$  is assigned to the  $\text{NH}_2$  bending mode, while such band in the pure dodecylamine is located at around  $1593\text{ cm}^{-1}$  [24]. The shift of this band after the intercalation of dodecylamine is primarily caused by the hydrogen bonds formed between the hydrogen atoms of  $\text{NH}_2$  groups and the oxygen atoms of silica tetrahedron during the intercalation process, which provides evidence that the  $\text{NH}_2$  groups play a key role for the intercalation action of the dodecylamine into kaolinite. In terms of the stretching vibration of  $\text{CH}_2$  groups of

pure dodecylamine at  $1466\text{ cm}^{-1}$  [24], this band splits to two bands at  $1493\text{ cm}^{-1}$  and  $1463\text{ cm}^{-1}$  respectively after the intercalation, as shown in Fig. 3, which may be explained as that a certain number of  $\text{CH}_2$  groups of intercalated dodecylamine hydrogen bonded to the silica tetrahedron. Therefore, it can be inferred that some intercalated dodecylamine molecules lie flat on the silica tetrahedron surface with their alkyl chains parallel to the kaolinite basal surface. The bands at  $2920\text{ cm}^{-1}$  and  $2848\text{ cm}^{-1}$  are primarily caused by the antisymmetric and symmetric C-H stretching motion of  $\text{CH}_3$  groups of adsorbed methanol molecules [20]. Additionally, a small band observed at around  $1646\text{ cm}^{-1}$  may be caused by the  $\text{NH}_3^+$  bending motion, implying that the protonated dodecylamine molecules may coexist with dodecylamine molecules in the interlayer space of kaolinite.

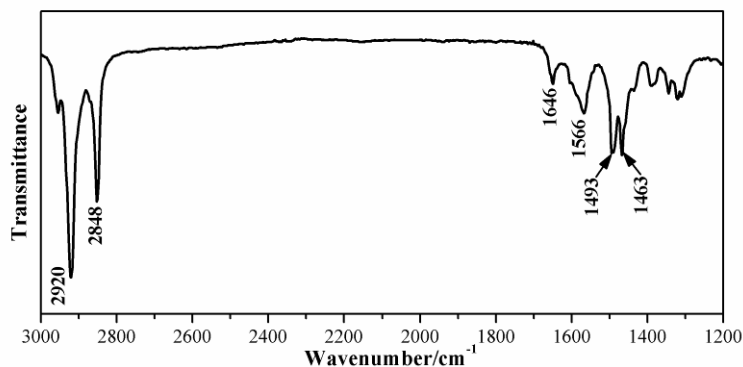


**Fig. 3.** FTIR spectrum of kaolinite-dodecylamine intercalation complex in the middle frequency region.

### 3.3. Molecular dynamics simulation analysis

The modified Dreiding force field has been proven to be suitable for the simulations of clay mineral-organic interactions by previous studies [2, 30, 45, 46]. The simulated

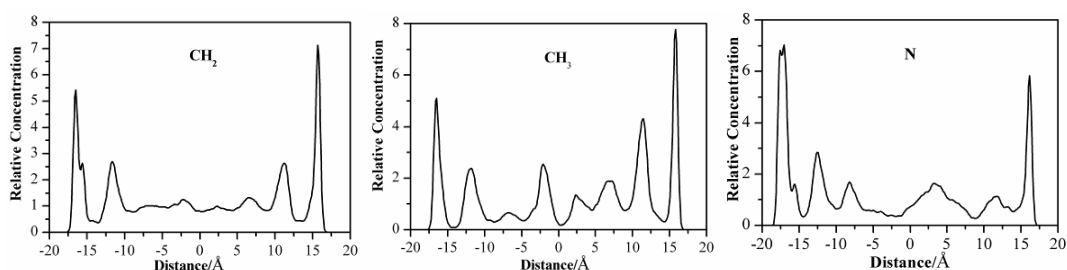


value of the basal spacing for the equilibrium structure of the kaolinite-dodecylamine system was obtained by averaging the final NPT simulation of 300 ps. In this study, a series of kaolinite-dodecylamine complex models with different numbers of dodecylamine molecules were built, and their basal spacing of equilibrium structure were calculated with the method mentioned above. The results indicated that the basal spacing of the equilibrium structure strongly depended on the number of intercalated dodecylamine molecules, and it presented a clear increase trend with an increase in the number of dodecylamine molecules. For the model of kaolinite intercalated with 45 dodecylamine molecules, the simulated basal spacing is 4.36 nm agreeing well with the experimental result (4.29 nm) obtained by XRD. Thus this complex model was chosen for a deep probe into the interface structure of kaolinite-dodecylamine intercalation complex in a molecular scale.

To establish the structure of intercalated dodecylamine in kaolinite gallery, the density distributions of its various components in the direction perpendicular to the clay basal surface were calculated. The concentration profiles of the N, methyl group and methylene group of intercalated dodecylamine molecules in the kaolinite-dodecylamine system, calculated on the basis of the final NPT simulation of 300 ps, are given in Fig. 4. The concentration profiles for all components in the system reveal a multi-layered distribution of intercalated dodecylamine. From N concentration profile, we can clearly see two sharp peaks in the position near to the silica tetrahedron surface and Alumina octahedron surface of kaolinite, indicating that

most head groups of intercalated dodecylamine reside in two layers close to surface of silica tetrahedron and alumina octahedron respectively. This result is due to the hydrogen bonding interaction between the O atoms of six-membered rings of the silica tetrahedron and the H atoms of head groups of the dodecylamine, and the hydrogen bonding interaction between the H atoms of hydroxyl of the opposing alumina octahedron and the N atoms of head groups of the dodecylamine, respectively. Apart from the two sharp peaks, some small peaks can also be noticed between them, revealing that some head groups also distribute throughout the accessible interlayer space in the system of kaolinite-dodecylamine. The concentration profile of the methyl group also presents two main sharp peaks in the same position as that for N group, as well as two secondary peaks next to them, demonstrating that a large proportion of methyl groups predominate four layers in the kaolinite gallery although they are present throughout the interlayer space on the basis of the presentation of some small peaks between the four main peaks. Notably, there is a middle peak appearing in the middle position of the interlayer space, which is attributed to the tail methyls of alkyl chain pushed toward the middle plane of interlayer space. The interlayer structure of kaolinite-dodecylamine intercalation complex can be further demonstrated by the concentration profile of the methylene group in the alkyl chain. There are two sharp peaks accompanied by two middle peaks perfectly symmetrically appearing near to the silica tetrahedron surface and Alumina octahedron surface, which indicates that most alkyl chains form four-layer structure , in which two of

them lie flat close to the silica tetrahedron surface and the other two lie flat close to the alumina octahedron surface. In addition to the four sharp peaks, some low-resolution smoothed peaks are present in the middle position of the interlayer space, which means the existence of a paraffin-type-like structure of the intercalated dodecylamine. Thus, a mixture of paraffin-type-like structure and two bilayer structures is more reasonable to explain the conformation of the intercalated dodecylamine.



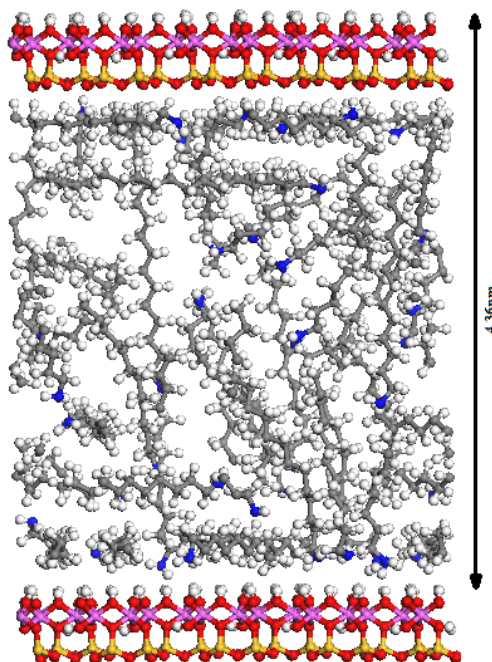
**Fig. 4.** Concentration profiles of the N, methyl group and methylene group of intercalated dodecylamine molecules. The origin is located at the middle plane of two kaolinite sheets.

Fig. 5 shows a snapshot of the simulation cell of kaolinite-dodecylamine complex model after the system reached equilibrium. It clearly demonstrates the layering behavior of the intercalated dodecylamine molecules within the interlayer space of kaolinite. The paraffin-type-like arrangement of intercalated dodecylamine is observed in the middle interlayer space of kaolinite. Additionally, two bilayer structures are observed near the silica tetrahedron surface and alumina octahedron surface respectively, in which the alkyl chains in each layer adopt an orientation with their longest axis approximately parallel to the kaolinite basal surface. In addition, a certain number of disordered chain configurations containing some gauche

conformers can also be seen, indicating that all-trans conformation of alkyl chains is hard to be identified from our simulated results.

In previous study on molecular conformation of the intercalated alkyl chains confined in the interlayer space of smectites[1, 47], the idealized structural models, such as pseudo-quadrilayers and paraffin-type monolayers and bilayers were inferred by the basal spacing of smectites-alkylammonium intercalation compounds investigated by XRD in conjunction with the alkyl chain length. However, an alternative arrangement based on a disordered chain configuration containing numerous gauche conformers would also be consistent with the observed basal spacings [48]. Thus determining the interlayer structure solely on XRD measurements is inadequate. Vaia et al. [48] used Transmission FTIR to probe the interlayer structure and phase state of intercalated alkylammonium silicates by monitoring frequency shifts of the CH<sub>2</sub> stretching and scissoring vibrations as a function of interlayer packing density, chain length, and temperature, and found that substantial disordered, gauche conformation of alkyl chains existed in most conditions. In addition, molecular dynamics simulation study on surfactant-modified montmorillonite such as alkylammoniums and dioctadecyldimethyl ammoniums reported by Zeng et al. [2, 30, 49] directly revealed the coexistence of ordered trans and disordered gauche conformations of intercalated guests. In our simulation case, the alkyl chains of intercalated dodecylamine also adopt a mixture of ordered and disordered configuration in the middle interlayer space of kaolinite, together with the bilayer arrangement near the silica tetrahedron surface

and alumina octahedron surface of kaolinite.



**Fig. 5.** Snapshot of the kaolinite-dodecylamine system after equilibrium is reached.

#### 4. Conclusions

Methanol was intercalated into the interlayer space of kaolinite by the treatment of washing the kaolinite-DMSO intercalation complex with fresh methanol repeatedly. Kaolinite-dodecylamine intercalation complex was synthesized by using the methanol treated kaolinite-DMSO intercalation complex as the intermediate. When the dodecylamine was intercalated into the kaolinite, its basal spacing, measured by XRD, expanded from 0.72 nm to 4.29 nm. The intercalation of kaolinite with dodecylamine was also confirmed by the FTIR spectra of prepared samples, in which the OH-stretching bands attributed to the inner surface hydroxyl of kaolinite changed profoundly. Additionally, some characteristic bands attributed to the groups of dodecylamine were also observed, the band at  $1566\text{ cm}^{-1}$  was assigned to the  $\text{NH}_2$

bending mode, and the bands at  $1493\text{ cm}^{-1}$  and  $1463\text{ cm}^{-1}$  were the  $\text{CH}_2$  stretching mode, for example. But these bands shifted to some degree compared to the pure dodecylamine, indicating that the  $\text{CH}_2$  and  $\text{NH}_2$  groups hydrogen bonded to the internal surface of kaolinite.

Molecular dynamics simulation was carried out to investigate the layering behavior and structure of nanoconfined dodecylamine in the kaolinite gallery. The simulated results indicated that alkyl chains within the interlayer space of kaolinite adopted a hybrid layering structure rather than the idealized structural models such as pseudo-trilayer or paraffin-type layer. The alkyl chains aggregated to a mixture of ordered paraffin-type-like structure and disordered gauche conformation in the middle interlayer space of kaolinite, and a certain number of alkyl chains arranged in two bilayer structures, in which one was near to the silica tetrahedron surface, and the other was near to the alumina octahedron surface with their alkyl chains parallel to the kaolinite basal surface.

## **Acknowledgments**

The authors gratefully acknowledge the financial support provided by the National Natural Science Foundation of China (51034006), the Beijing Joint-Construction Project (20121141301).

## References

- [1] G. Lagaly, M. Ogawa, I. Dékány, *Developments in Clay Science* 1 (2006) 309.
- [2] Q. Zeng, A. Yu, G. Lu, R. Standish, *Chemistry of Materials* 15 (2003) 4732.
- [3] E.P. Giannelis, *Advanced Materials* 8 (1996) 29.
- [4] C. Kaynak, G.I. Nakas, N.A. Isitman, *Applied Clay Science* 46 (2009) 319.
- [5] P.C. LeBaron, Z. Wang, T.J. Pinnavaia, *Applied Clay Science* 15 (1999) 11.
- [6] E. Manias, A. Touny, L. Wu, K. Strawhecker, B. Lu, T. Chung, *Chemistry of Materials* 13 (2001) 3516.
- [7] S. Sinha Ray, P. Maiti, M. Okamoto, K. Yamada, K. Ueda, *Macromolecules* 35 (2002) 3104.
- [8] Y.Y. Leu, Z.A. Mohd Ishak, W.S. Chow, *Journal of Applied Polymer Science* 124 (2012) 1200.
- [9] M. Pluta, J.K. Jeszka, G. Boiteux, *European Polymer Journal* 43 (2007) 2819.
- [10] T.M. Wu, C.Y. Wu, *Polymer Degradation and Stability* 91 (2006) 2198.
- [11] É. Makó, J. Kristóf, E. Horváth, V. Vágvolgyi, *Journal of Colloid and Interface Science* 330 (2009) 367.
- [12] H. Cheng, Q. Liu, J. Yang, S. Ma, R.L. Frost, *Thermochimica Acta* 545 (2012) 1.
- [13] P. Costanzo, R. Giesse, *Clays and Clay Minerals* 34 (1986) 105.
- [14] B. THENG, *Clays and Clay Minerals* 32 (1984) 241.
- [15] M.D.R. Cruz, F. Franco, *Clays and Clay Minerals* 48 (2000) 63.
- [16] R.L. Frost, J. Kristof, E. Horvath, J.T. Klopogge, *Journal of Colloid and Interface Science* 226 (2000) 318.
- [17] H. Cheng, Q. Liu, J. Yang, Q. Zhang, R.L. Frost, *Thermochimica Acta* 503–504 (2010) 16.
- [18] H. Cheng, J. Yang, R. Frost, Q. Liu, Z. Zhang, *Journal of Thermal Analysis and Calorimetry* 103 (2011) 507.
- [19] H. Cheng, Q. Liu, J. Zhang, J. Yang, R.L. Frost, *Journal of Colloid and Interface Science* 348 (2010) 355.
- [20] P. Yuan, D. Tan, F. Annabi-Bergaya, W. Yan, D. Liu, Z. Liu, *Applied Clay Science* 83 (2013) 68.
- [21] J. Matusik, Z. Kłapyta, *Applied Clay Science* 83 (2013) 433.
- [22] Y. Kuroda, K. Ito, K. Itabashi, K. Kuroda, *Langmuir* 27 (2011) 2028.
- [23] J. Gardolinski, G. Lagaly, *Clay Minerals* 40 (2005) 547.
- [24] Y. Komori, Y. Sugahara, K. Kuroda, *Applied Clay Science* 15 (1999) 241.
- [25] Y. Komori, Y. Sugahara, K. Kuroda, *Journal of Materials Research* 13 (1998) 930.
- [26] Q. Fang, S. Huang, W. Wang, *Chemical Physics Letters* 411 (2005) 233.
- [27] G. Rutkai, T. Kristóf, *Chemical Physics Letters* 462 (2008) 269.
- [28] G. Rutkai, É. Makó, T. Kristóf, *Journal of Colloid and Interface Science* 334 (2009) 65.
- [29] R. Young, A. Hewat, *Clays and Clay Minerals* 36 (1988) 225.
- [30] Q. Zeng, A. Yu, G. Lu, R. Standish, *The Journal of Physical Chemistry B* 108

(2004) 10025.

[31] A.K. Rappe, W.A. Goddard III, *The Journal of Physical Chemistry* 95 (1991) 3358.

[32] Accelrys Inc. Materials studio 4.1 software. San Diego (CA), USA.

[33] R.L. Frost, É. Makó, J. Kristóf, J.T. Klopogge, *Spectrochimica Acta Part A: Molecular and Biomolecular Spectroscopy* 58 (2002) 2849.

[34] J. Kristó, R.L. Frost, A. Felinger, J. Mink, *Journal of Molecular Structure* 410–411 (1997) 119.

[35] R.L. Frost, E. Horváth, É. Makó, J. Kristóf, *Journal of Colloid and Interface Science* 270 (2004) 337.

[36] R.L. Frost, J. Kristof, E. Horvath, J.T. Klopogge, *Journal of Colloid and Interface Science* 214 (1999) 109.

[37] J.J. Tunney, C. Detellier, *Journal of Materials Chemistry* 6 (1996) 1679.

[38] J.J. Tunney, C. Detellier, *Chemistry of Materials* 5 (1993) 747.

[39] C.T. Johnston, G. Sposito, D.F. Bocian, R.R. Birge, *The Journal of Physical Chemistry* 88 (1984) 5959.

[40] R.L. Frost, J. Kristof, G.N. Paroz, J.T. Klopogge, *The Journal of Physical Chemistry B* 102 (1998) 8519.

[41] W.N. Martens, R.L. Frost, J. Kristof, E. Horvath, *The Journal of Physical Chemistry B* 106 (2002) 4162.

[42] Y. Zhang, Q. Liu, Z. Wu, Q. Zheng, H. Cheng, *Journal of Thermal Analysis and Calorimetry* 110 (2012) 1167.

[43] J. Tunney, C. Detellier, *Clays and Clay Minerals* 42 (1994) 473.

[44] Y. Komori, H. Enoto, R. Takenawa, S. Hayashi, Y. Sugahara, K. Kuroda, *Langmuir* 16 (2000) 5506.

[45] G. Tanaka, L.A. Goettler, *Polymer* 43 (2002) 541.

[46] S.P. Newman, T. Di Cristina, P.V. Coveney, W. Jones, *Langmuir* 18 (2002) 2933.

[47] G. Lagaly, *Solid State Ionics* 22 (1986) 43.

[48] R.A. Vaia, R.K. Teukolsky, E.P. Giannelis, *Chemistry of Materials* 6 (1994) 1017.

[49] Q. Zeng, A. Yu, G.M. Lu, *Nanotechnology* 16 (2005) 2757.



## LIST OF FIGURES

**Fig. 1.** XRD patterns of (a) original kaolinite, (b) kaolinite-DMSO intercalation complex, (c) kaolinite-methanol intercalation complex, (d) kaolinite-dodecylamine intercalation complex, and (e) crystalline dodecylamine.

**Fig. 2.** FTIR spectra of (a) kaolinite, (b) kaolinite-DMSO intercalation complex, (c) methanol-treated kaolinite-DMSO intercalation complex, and (d) kaolinite-dodecylamine intercalation complex in the high frequency region.

**Fig. 3.** FTIR spectrum of kaolinite-dodecylamine intercalation complex in the middle frequency region.

**Fig. 4.** Concentration profiles of the N, methyl group and methylene group of intercalated dodecylamine molecules. The origin is located at the middle plane of two kaolinite sheets.

**Fig. 5.** Snapshot of the kaolinite-dodecylamine system after equilibrium is reached.

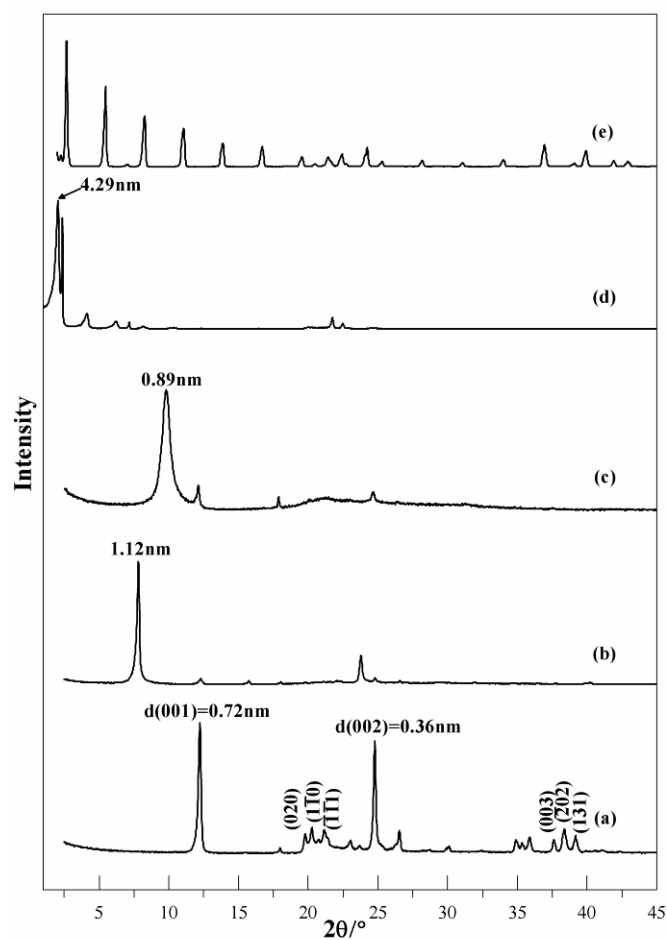


**Fig. 1.** XRD patterns of (a) original kaolinite, (b) kaolinite-DMSO intercalation complex, (c) kaolinite-methanol intercalation complex, (d) kaolinite-dodecylamine intercalation complex, and (e) crystalline dodecylamine.

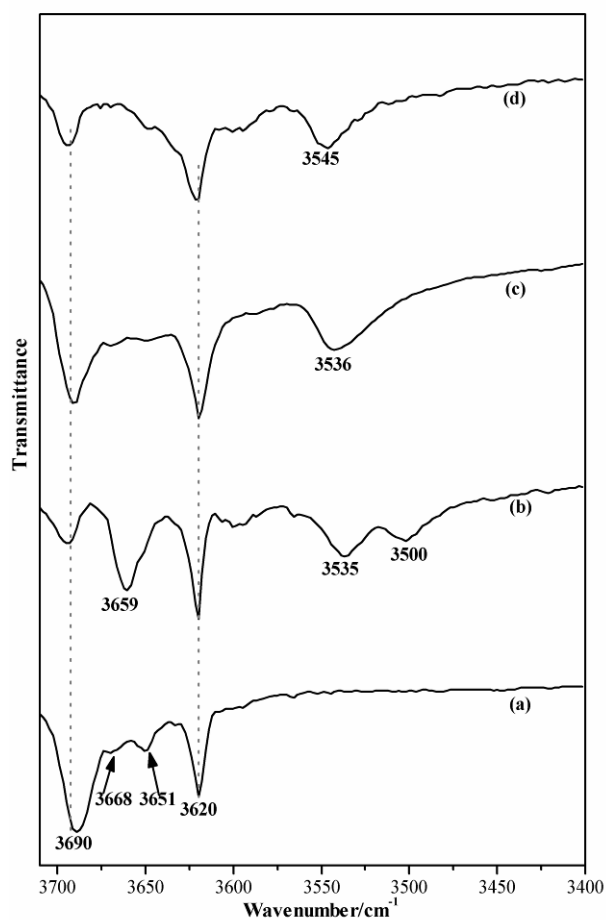


**Fig. 2.** FTIR spectra of (a) kaolinite, (b) kaolinite-DMSO intercalation complex, (c) methanol-treated kaolinite-DMSO intercalation complex, and (d) kaolinite-dodecylamine intercalation complex in the high frequency region.

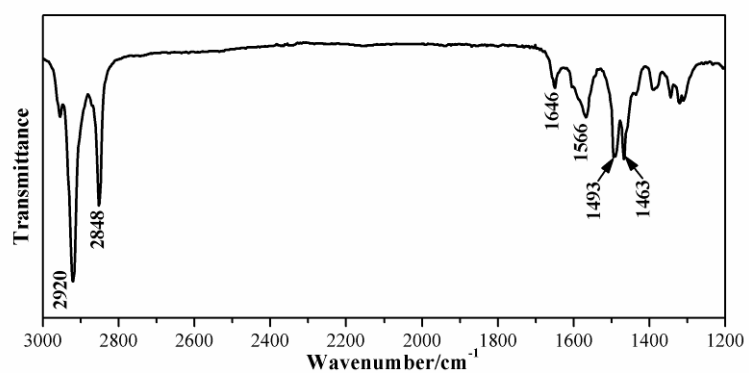


**Fig. 3.** FTIR spectrum of kaolinite-dodecylamine intercalation complex in the middle frequency region.

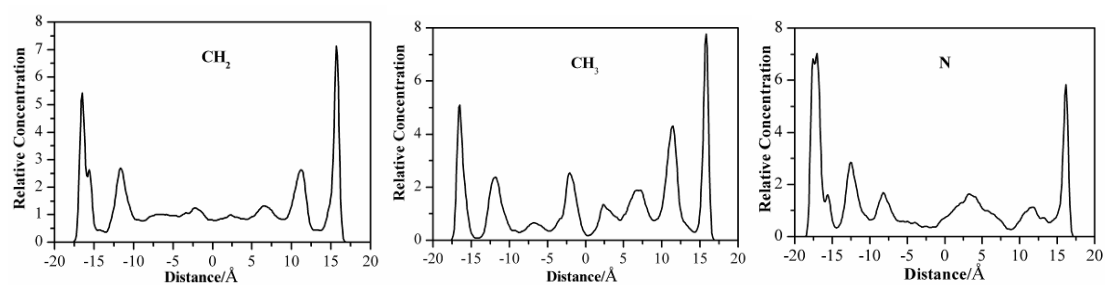


**Fig. 4.** Concentration profiles of the N, methyl group and methylene group of intercalated dodecylamine molecules. The origin is located at the middle plane of two kaolinite sheets.

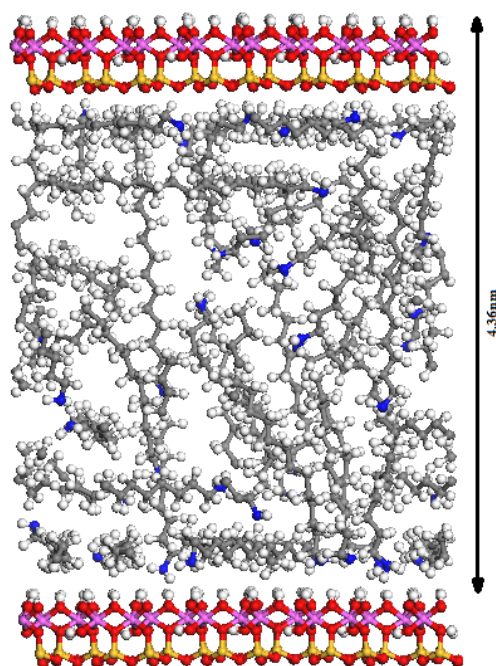


**Fig. 5.** Snapshot of the kaolinite-dodecylamine system after equilibrium is reached.